Transitional nonlinear elastic behaviour in dense granular media

Thomas Brunet,[1] Xiaoping Jia,[1] and Paul A. Johnson[1,2]

Received 7 July 2008; revised 26 August 2008; accepted 28 August 2008; published 11 October 2008.

[1] Nonlinear sound propagation in a stressed glass bead pack is investigated via amplitude measurements of harmonic generation. We evidence two distinct regimes of sound-matter interaction: reversible and irreversible, as a function of the ratio r_s between dynamic strain and static one. In the reversible regime, the higher harmonics generated agree well with a mean-field model based on the Hertz contact theory, and the coefficient of nonlinearity β deduced from the measured amplitude of second-harmonic is consistent with that deduced from the acoustoelastic measurement. Beyond a certain threshold ($r_s > 3\%$), the interaction of sound wave with granular matter becomes irreversible, accompanied by a small compaction of the medium. **Citation:** Brunet, T., X. Jia, and P. A. Johnson (2008), Transitional nonlinear elastic behaviour in dense granular media, *Geophys. Res. Lett.*, *35*, L19308, doi:10.1029/2008GL035264.

1. Introduction

[2] In a dense granular packing (solid volume fraction $\phi_S > 0.57$) the salient mechanical properties such as arching and slow dense flow are determined by the inhomogeneous internal stress fields [*Jaeger et al.*, 1996]. Small-amplitude sound propagation, coherent and multiply scattered, provides an efficient and non intrusive probe for characterizing the structure and viscoelastic properties of granular materials [*Liu and Nagel*, 1993; *Jia et al.*, 1999]; however, the nonlinear elastic behaviour of the materials become progressively more important at high-amplitude wave excitation. In ordinary elastic media, finite-amplitude sound propagation has been intensively studied to understand many nonlinear acoustic effects such as cumulative wave distortion with propagation distance as well as the concept of the parametric array [*Hamilton and Blackstock*, 1998]. Similar to rocks [*Guyer et al.*, 1997; *Van Den Abeele et al.*, 2002] and soils [*Lu*, 2005; *Gilcrist et al.*, 2007] non cohesive granular materials exhibit intense static and dynamic nonlinear behaviours, including strong acousto-elastic effects, dynamic wave hysteresis and dynamic modulus softening [*Liu and Nagel*, 1993; *Johnson and Jia*, 2005]. Indeed the contact force network at low confining effective pressure is fragile and may be reorganized when subject to high-amplitude sound propagation [*Liu and Nagel*, 1993]. However, the physics underlying these nonlinear behaviours still remains unclear and the theory deduced from first-principle calculations is not available for such disordered media. Recently a clapping model based on the Hertz contact theory was proposed to describe wave demodulation in granular media [*Tournat et al.*, 2004]. Such a reversible mechanism of opening and closing of contacts has been widely employed in fissured heterogeneous materials, but may be less appropriate in granular materials where irreversible rearrangements of beads and their contacts should occur during clapping, consequently loosening the contacts with neighbours.

[3] In this Letter, we investigate nonlinear wave-amplitude dynamics in a glass bead pack under external stress by measuring higher harmonics generated as a function of the source amplitude. We test the applicability of the Hertz contact theory to the granular systems at moderate amplitude and determine the coefficient of nonlinearity β both from higher harmonics generated and from acoustoelastic measurements. The different regimes of sound-granular matter interaction are also explored in terms of reversibility. This work may provide a useful laboratory model for better understanding the large-scale field experiments such as nonlinear sediment response during strong ground motion. [*Lu*, 2005; *Gilcrist et al.*, 2007].

2. Experiments and Results

[4] Our dry granular media are composed of polydisperse glass beads of diameter d = 0.6–0.8 mm, confined in a cylinder of diameter 60 mm and closed by two fitted pistons ($\phi_S \approx 0.63$). We apply a normal load P_0 of several hundred *kPa* to the medium after one cycle of loading-unloading. Lengths of the cell L range from 25 mm to 65 mm. A broadband source transducer of diameter 30 mm and an identical detecting transducer are placed on the axis, respectively, at the top and bottom of the cell in direct contact with glass beads. A ten-cycle tone burst excitation centered at f (= $\omega/2\pi$) = 50 kHz is applied to the source transducer. At low frequency ($\lambda \gg d$) as in this work, longitudinal waves undergo coherent propagation. By using an impedance matched power amplifier (ENI), the measured amplitude of source displacement u_{in} by an optical interferometer ranges from 2.5 to 62.5 nm.

[5] In Figure 1a, we present the typical transmitted waveform detected at a distance of 64 mm under the confining pressure P_0 = 720 kPa. The sound velocity is measured as c_0 = 900 m/s by the time of flight, and the source amplitude is $u_{in} \approx 62.5$ nm corresponding to the dynamic strain ε_{in} (= $\omega u_{in}/c_0$) $\approx 2\ 10^{-5}$. To study the generation of higher harmonics, we band-pass filtered the output signal using a temporal numerical filter centred at 50 kHz, 2 × 50 kHz and 3 × 50 kHz, respectively (Figures 1b–1d). The amplitudes of the fundamental, second harmonic are then measured as a function of the source amplitude ε_{in}. These data fit well a linear and quadratic power-law dependence on ε_{in} (solid lines) over our experimental range, as illustrated on log-scale in Figure 1 (insets). The third harmonic

[1] LPMDI, Université Paris-Est, CNRS UMR8108, Marne la Vallée, France.

[2] On leave from Los Alamos National Laboratory, Los Alamos, New Mexico, USA.

0094-8276/08/2008GL035264$05.00

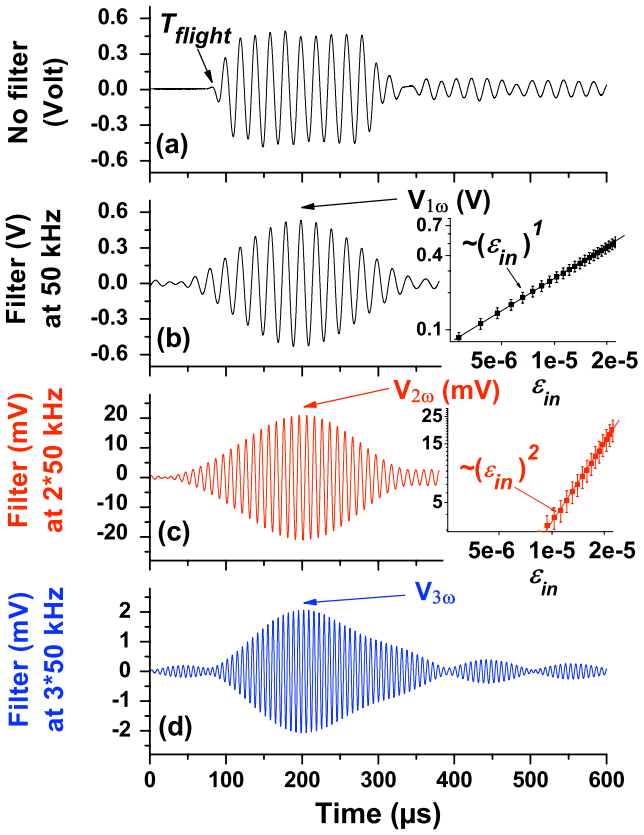

Figure 1. (a) Transmitted ultrasonic wave-trains and the filtered (b) fundamental component $V_{1\omega}$, (c) second harmonic $V_{2\omega}$ and (d) third harmonic $V_{3\omega}$ under P_0 = 720 kPa. Inset: Amplitudes $V_{1\omega}$, $V_{2\omega}$ vs ε_{in}.

is present, but the data is much scattered because of poor signal/noise ratio (not shown). This test, together with the attenuation measurements described below (Figure 3), demonstrates a classic nonlinear behaviour like that observed in ordinary elastic materials, although much larger in magnitude, and ensure that the nonlinearity from the parasite sources (e.g. electrical equipment) is negligible in our experiments. Over the amplitude range shown in Figure 1, no amplitude hysteresis is observed when ε_{in} is increased and subsequently decreased, pointing to a reversible process.

[6] We next investigate the nonlinear behaviour evolution of the granular medium as we decrease the confining pressure P_0. Figure 2 shows that the fundamental and the second-harmonic amplitudes depart significantly from the linear or quadratic dependence on ε_{in} above a threshold depending on P_0. For P_0 = 180 kPa the deviation from the classical scaling of the power-law (Figures 2a and 2b) is observed at $\varepsilon_{in} \approx 7.5\ 10^{-6}$. A small compaction induced of about 20 μm is also simultaneously detected by a sensor with 1 μm in resolution above this threshold (Figure 2c). This observation indicates the irreversible nature of the nonlinear behaviour in this amplitude range. The same experiments were conducted for P_0 = 90 kPa and P_0 = 360 kPa where transition occurs around $\varepsilon_{in} \approx 4.5\ 10^{-6}$ and $12\ 10^{-6}$, respectively. In terms of the static compression ε_0 ($\sim P_0^{2/3}$ according to the Hertz elasticity, see below), the threshold ε_{in} corresponds roughly to a dimensionless ratio $r_s = \varepsilon_{in}/\varepsilon_0$ of about 3%. These results suggest a possible transition diagram as a function of r_s (Figure 2c, inset) between two distinct regimes of sound-matter interaction.

3. Analysis and Discussion

[7] In order to interpret the nonlinear behaviour observed in the reversible regime, we analyze our results with a mean-field model based on the Hertz contact nonlinearity. Denote σ_a and ε_a as dynamic stress and strain, respectively, the stress-strain relation can be expressed by

$$\sigma_a = K_0\varepsilon_a(1 + \beta\varepsilon_a + \ldots) + \eta\frac{\partial\varepsilon_a}{\partial t} \quad (1)$$

where K_0 is the linear dynamic modulus related to the sound velocity $c_0 = \sqrt{(K_0/\rho_0)}$, and β is the coefficient of nonlinearity also termed as the third-order elastic constant - the principal measure of the finite-amplitude distortions associated with the sound propagation. As shown below, β can be determined by either wave mixing measurements (e.g., harmonic generation) or acoustoelastic measurements. As a first approach to account for the internal dissipation in the granular medium, we add a loss term via η, akin to the viscosity in fluids, which leads to the Burgers equation -the most widely used model equation for studying the combined effects of attenuation and nonlinearity on progressive plane waves [*Hamilton and Blackstock*, 1998]:

$$\rho_0\frac{\partial^2 u}{\partial t^2} - \eta\frac{\partial^3 u}{\partial a^2\partial t} - \rho_0 c_0^2\frac{\partial^2 u}{\partial a^2} - 2\rho_0 c_0^2\beta\left(\frac{\partial u}{\partial a}\right)\left(\frac{\partial^2 u}{\partial a^2}\right) = 0 \quad (2)$$

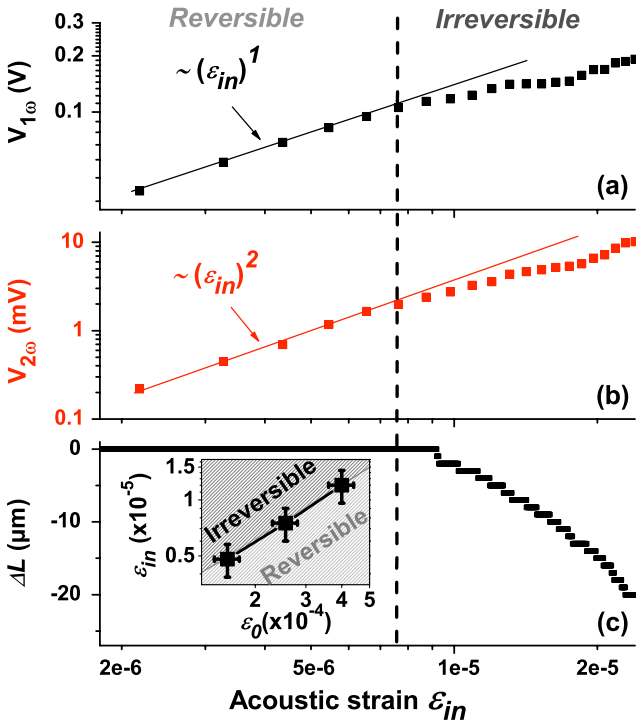

Figure 2. (a) Fundamental component $V_{1\omega}$ and (b) second harmonic $V_{2\omega}$ amplitudes vs source amplitude ε_{in} under P_0 = 180 kPa, together with (c) the sample height variation ΔL. Solid lines correspond to classical nonlinear predictions. Inset: transition diagram ε_{in} vs ε_0.

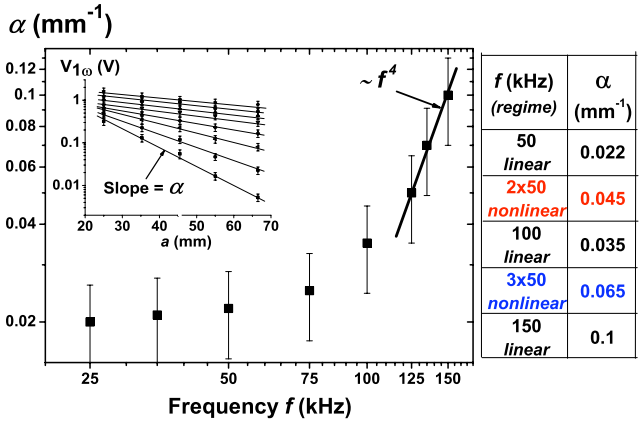

f (kHz) (regime)	α (mm^{-1})
50 linear	0.022
2x50 nonlinear	0.045
100 linear	0.035
3x50 nonlinear	0.065
150 linear	0.1

Figure 3. Linear attenuation coefficient α vs f. Inset: fundamental amplitudes $V_{1\omega}$ vs distance a for different frequency f, measured under $P_0 = 720$ kPa with $u_{in} = 62.5$ nm. Solid lines correspond to linear fits. Table: Attenuation coefficient measured in both linear and nonlinear regimes.

where ρ_0 is the medium density and a is the material coordinate.

[8] Introducing the Gold'berg number $\Gamma = l_A/l_S$ defined as the ratio of the attenuation length to the shock distance, we can obtain the approximate expressions for the displacement fields in the limiting case of weak waves dominated by the attenuation process ($\Gamma < 1$). Remember that $l_A = 1/\alpha$ where α is the linear coefficient of attenuation and $l_S = 1/(\beta k \varepsilon_{in})$ where k is the wave number. If the distance of propagation a is comparable or larger than l_A (i.e., $a\alpha \geq 1$), the displacements of the fundamental, second and third harmonic components can be further simplified, as:

$$u_{1\omega}(a,t) \approx u_{in} e^{-\alpha a} \cos(ka - \omega t) \tag{3a}$$

$$u_{2\omega}(a,t) \approx \frac{u_{in}^2}{8} \left(\frac{\beta\omega^2}{\alpha c_0^2}\right) e^{-2\alpha a} \cos 2(ka - \omega t) \tag{3b}$$

$$u_{3\omega}(a,t) \approx \frac{u_{in}^3}{48} \left(\frac{\beta\omega^2}{\alpha c_0^2}\right)^2 e^{-3\alpha a} \cos 3(ka - \omega t) \tag{3c}$$

with $\alpha = \eta\omega^2/(2\rho_0 c_0^3)$. Notice that the approximate expressions given in equation (3) would have a more general use which is not limited by the specific loss model in equation (1) [*McCall*, 1994], provided that α is determined independently, e.g., by measurements.

[9] To this end, we measure the amplitudes of the transmitted signals ($V_{1\omega}$) as a function of distance a at small-amplitude input for different frequency f. As shown in Figure 3 (inset), the amplitude dependences are linear in the semi-logarithmic scale and the slopes of the straight lines provide the linear attenuation coefficients $\alpha(f)$. The same measurements of α are conducted in the nonlinear regime with the second and third harmonics, respectively. Several results are given in Figure 3 (table). The observation that $\alpha_{2*50\text{kHz}} \neq \alpha_{100\text{kHz}}$ and $\alpha_{3*50\text{kHz}} \neq \alpha_{150\text{kHz}}$ confirms that the harmonic generation observed in our experiments arises within the granular medium and not from the parasite sources originating at the input level. Moreover, the data show that $\alpha_{2*50\text{kHz}} \approx 2\alpha_{50\text{kHz}}$ and $\alpha_{3*50\text{kHz}} \approx 3\alpha_{50\text{kHz}}$, which is reasonably in agreement with the predictions of equations (3) and consequently supports the validity of the present model. For $f = 50$ kHz the attenuation length l_A is about 45 mm; the observation of second-harmonic growth occurring principally within $a < 10$ mm is difficult, if not impossible, with our granular samples for a/d is only about 15 (Figure 3, inset). Note that the understanding of the internal dissipation mechanism in the granular medium still remains incomplete; it most likely depends on the interplay between frictional, viscoelastic and scattering losses [*Brunet et al.*, 2008], implying a complex behaviour of $\alpha(f)$ (Figure 3).

[10] With the attenuation α measured in the granular packing under $P_0 = 720$ kPa, we can deduce the coefficient of nonlinearity β from the ratio of measured second-harmonic amplitude to fundamental one shown in Figures 1b and 1c (insets), $V_{2\omega}/V_{1\omega}$ ($=u_{2\omega}/u_{1\omega}$) according to equations (3a) and (3b). The difficulty of the wave mixing method is that an independent measurement of u_{in} is required. If the displacement of the source transducer measured at its free surface is considered, we obtain $\beta_{WM} \approx 3000$. This gives a shock wave distance l_S of about few meters much larger than l_A, verifying the condition $\Gamma < 1$ assumed.

[11] The most commonly used and the most precise method for determining β is based on the acoustoelastic effect, namely *velocity measurement*, in which the application of a static stress P_0 change the velocity c_0 of small-amplitude sound waves as $\beta_{AE} = (\rho_0/2)(dc_0^2/dP_0)$. Figure 4 displays the sound velocity measured by a time-of-flight method as a function of the applied stress. The power-law scaling $c_0 \sim P_0^{0.15}$ agrees well with the prediction by the Hertz theory $c_0 \sim P_0^{1/6}$ [*Jia et al.*, 1999]. The coefficient of nonlinearity β_{AE} is then deduced by differentiating the sound velocity. The results shown in Figure 4 reveal a reasonably good agreement between measured β_{AE} and the predicted $\beta_{Hertz} = 1/(4\varepsilon_0)$ [*Norris and Johnson*, 1997], thus confirming the primary role of the Hertz nonlinearity in the granular nonlinear elasticity. Further-

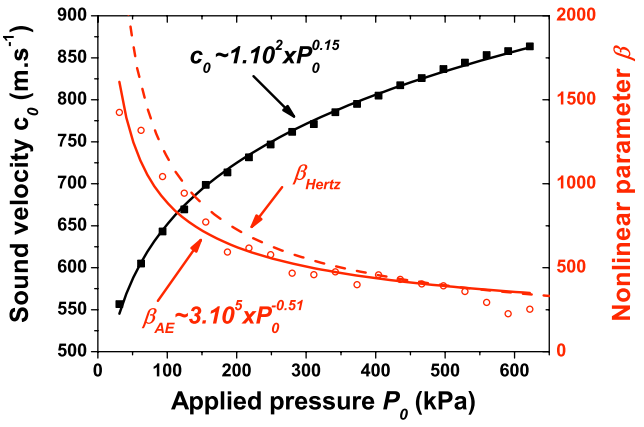

Figure 4. Solid squares are sound velocity c_0 measured vs P_0, and open circles are β_{AE} deduced from velocity measurements. Solid lines correspond to power law fits and dashed line refers to calculated values β_{Hertz} from the Hertz contact model.

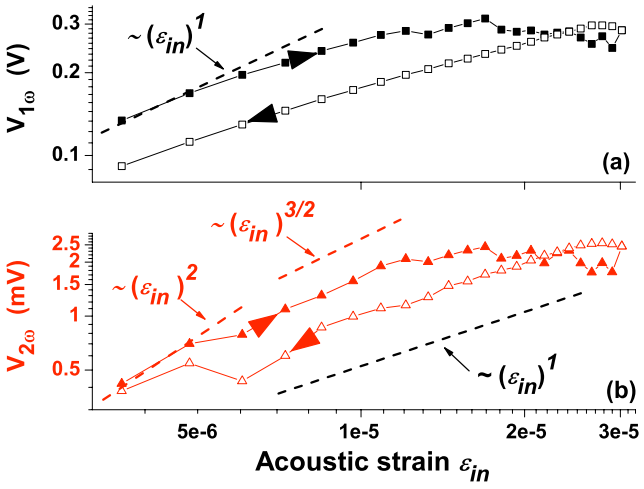

Figure 5. (a) Fundamental and (b) second-harmonic amplitudes vs source amplitude ε_{in} under P_0 = 90 kPa. The curves correspond to increasing ε_{in} (solid symbols) and subsequently decreasing ε_{in} (open symbols).

more $\beta_{AE} \approx 350$ measured at P_0 = 720 kPa gives $\beta_{WM} \approx 8\beta_{AE}$. The discrepancy between β values obtained by the two methods is also reported in sedimentary rocks [*D'Angelo et al.*, 2004].

[12] Let us finally examine the irreversible regime lower confining pressure. In Figure 5, the fundamental component and second harmonics demonstrate non-classical behaviours, i.e. amplitude hysteresis and the important deviation of the source-amplitude ε_{in} dependence from the classical scaling laws illustrated in Figure 1. The scaling with ε_{in} in our experiments is not determinate and depends strongly on the confining pressure and the sample preparation procedure. The observation of such amplitude dynamics is similar to those in previous experiments [*Liu and Nagel*, 1993], and clearly reveals that there is no evidence for a scaling law such as $\varepsilon_{in}^{3/2}$ for the second harmonic generation, predicted by the clapping model [*Tournat et al.*, 2004]. In fact, the reversible nature of such a mechanism is inconsistent with the observed hysteretic behaviour and the irreversible compaction induced in this regime. Notice, however, the characteristic length scale associated with this small plastic deformation is different from that observed in a tapping experiment [*Nowak et al.*, 1998]. Instead, it is probably related to frictional dynamics at the grain contact level, leading to the onset of the micro-arrangement of asperities between rough spheres and resulting in a softening of elastic modulus and a change in the morphology of the contact networks (to be detailed elsewhere). This picture is consistent with the observed small threshold value r_s of a few percent. We believe that our work bridges the nonlinear sound-matter interaction described here and the recent concept of effective granular temperature (energy injected by vibration) proposed in the jamming transition process.

4. Conclusions

[13] In summary, we have identified two regimes of nonlinear elastic behaviour in a confined granular medium stemming from the nonlinear dynamics at the grain contacts. At moderate amplitudes we find a reversible process of the sound-material interaction where the second and third harmonic generation agree with the granular elasticity predicted by the Hertz contact theory. In this regime, sound speed measurements allow us to determine the coefficient of nonlinearity β in agreement with the model. Beyond threshold amplitude corresponding to r_s about a few percent, the irreversible process of sound-matter interaction commences and the pure Hertz model is no longer valid. Our experiments show that interpretations based only on the Hertzian nonlinear elasticity are incomplete for describing the granular nonlinear dynamics, and the frictional dynamics at the grain contact level should be included [*Nihei et al.*, 2000]. In studies of strong ground motion, it is clear that these hysteretic behaviours may play an important role; however, the effects of grain's shape and size dispersion as well as lower confining pressure condition should be considered in the future work.

[14] **Acknowledgment.** We thank R. A. Guyer for the very helpful comments and discussions and J. Laurent for the assistances. P. A. J. acknowledges the visiting-scientist position of the CNRS-FRANCE, and Institutional Support (LDRD) at Los Alamos.

References

Brunet, T., X. Jia, and P. Mills (2008), Mechanisms of acoustic absorption in dry and weakly wet granular media, *Phys. Rev. Lett.*, *101*, 138001(1–4).

D'Angelo, R. M., K. W. Winkler, T. J. Plona, B. J. Landsberger, and D. L. Johnson (2004), Test of hyperelasticity in highly nonlinear solids: Sedimentary rocks, *Phys. Rev. Lett.*, *93*, 214301, doi:10.1103/PhysRevLett.93.214301.

Gilcrist, L. E., G. S. Baker, and S. Sen (2007), Preferred frequencies for three unconsolidated Earth materials, *Appl. Phys. Lett.*, *91*, 254103, doi:10.1063/1.2820606.

Guyer, R. A., K. R. McCall, G. N. Boitnott, L. B. Hilbert Jr., and T. J. Plona (1997), Quantitative implementation of Preisach-Mayergoyz space to find static and dynamic elastic moduli in rock, *J. Geophys. Res.*, *102*, 5281–5293.

Hamilton, M., and D. Blackstock (1998), *Nonlinear Acoustics*, Academic, San Diego, Calif.

Jaeger, H. M., S. R. Nagel, and R. P. Behringer (1996), Granular solids, liquids and gases, *Rev. Mod. Phys.*, *68*, 1259–1273.

Jia, X., C. Caroli, and B. Velicky (1999), Ultrasound propagation in externally stressed granular media, *Phys. Rev. Lett.*, *82*, 1863–1866.

Johnson, P. A., and X. Jia (2005), Nonlinear dynamics, granular media and dynamic earthquake triggering, *Nature*, *437*, 871–873.

Liu, C. H., and S. R. Nagel (1993), Sound in a granular material: Disorder and nonlinearity, *Phys. Rev. B.*, *48*, 15,646–15,650.

Lu, Z. (2005), Role of hysteresis in propagating acoustic waves in soils, *Geophys. Res. Lett.*, *32*, L14302, doi:10.1029/2005GL022980.

McCall, K. R. (1994), Theoretical study of nonlinear elastic wave propagation, *J. Geophys. Res.*, *99*, 2591–2600.

Nihei, K. T., et al. (2000), Frictional effects on the volumetric strain of sandstones, *Int. J. Rock Mech. Min. Sci.*, *37*, 121–132.

Norris, A. N., and D. L. Johnson (1997), Nonlinear elasticity of granular media, *J. Appl. Mech.*, *64*, 39–49.

Nowak, E. R., et al. (1998), Density fluctuations in vibrated granular materials, *Phys. Rev. E.*, *57*, 1971–1982.

Tournat, V., et al. (2004), Probing granular media by acoustic parametric emitting antenna: Weak contacts, nonlinear dilatancy and polarization anisotropy, *Phys. Rev. Lett.*, *92*, 085502, doi:10.1103/PhysRevLett.92.085502.

Van Den Abeele, K. E.-A., J. Carmeliet, P. A. Johnson, and B. Zinszner (2002), Influence of water saturation on the nonlinear elastic mesoscopic response in Earth materials and the implications to the mechanism of nonlinearity, *J. Geophys. Res.*, *107*(B6), 2121, doi:10.1029/2001JB000368.

T. Brunet and X. Jia, LPMDI, Université Paris-Est, CNRS UMR8108, Cité Descartes, F-77454 Marne la Vallée, France. (jia@univ-mlv.fr)

P. A. Johnson, Los Alamos National Laboratory, NM 87545, USA.